

Stochastic Acceleration in the Galactic Center HESS Source

Siming Liu,¹ Fulvio Melia,^{2,3} Vahé Petrosian,⁴ and Marco Fatuzzo⁵

ABSTRACT

Stochastic acceleration of charged particles interacting resonantly with a turbulent magnetic field in a small accretion torus appears to be the likely mechanism responsible for much of Sagittarius A*'s mm and shorter wavelength spectrum. The longer wavelength radiation is produced at larger radii by electrons either diffusing from smaller scales or accelerated *in situ*. An important prediction of this model is the ejection of a significant flux of relativistic protons from a magnetic-field-dominated acceleration site into the wind-shocked medium surrounding the black hole. Recently, several air Čerenkov telescopes, notably HESS, have detected TeV emission from within 1' of the Galactic Center, with characteristics hinting at a pp-induced pion decay process for the γ -ray emission. Given (i) that we now know the size of this acceleration region, where Sagittarius A*'s 7-mm wavelength emission originates, and (ii) that we can now map the wind-injected ISM within ~ 3 pc of the nucleus using the diffuse X-rays detected with *Chandra*, it is feasible to test the idea that protons accelerated within ~ 20 Schwarzschild radii of the black hole produce the TeV emission farther out. We show that the diffusion length of these particles away from their source guarantees a majority of TeV protons scattering about once within ~ 3 pc of Sagittarius A*, and we demonstrate that the proton power ($\sim 10^{37}$ ergs s⁻¹) produced in concert with the 7-mm radio emission matches the TeV luminosity well. The particle cascade generated by the pp scatterings produces GeV γ -rays from π^0 decays, and bremsstrahlung, inverse Compton, and synchrotron emission at longer wavelengths from secondary particles. We compare these with current measurements and demonstrate that GLAST will detect this source during its

¹Los Alamos National Laboratory, Los Alamos, NM, 87545; liusm@lanl.edu

²Physics Department and Steward Observatory, The University of Arizona, Tucson, AZ 85721; melia@physics.arizona.edu

³Sir Thomas Lyle Fellow and Miegunyah Fellow.

⁴Center for Space Science and Astrophysics, Department of Applied Physics, Stanford University, Stanford, CA 94305; vahe@astronomy.stanford.edu

⁵Physics Department, Xavier University, Cincinnati, OH 45207

one-year all-sky survey. This model explains why the TeV source is unresolved, yet does not vary on a time scale of a year or less, and it also accounts for the high-energy emission while retaining consistency with Sgr A*'s well-studied cm and mm characteristics.

Subject headings: acceleration of particles — black hole physics — Galaxy: center — plasmas — turbulence

1. Introduction

Sagittarius A*, the compact radio source associated with the supermassive black hole (of mass $M \sim 3.4 \times 10^6 M_\odot$; Schödel et al. 2003, Ghez et al. 2003) at the Galactic Center, has a stratified emission structure in which the higher frequency emission is produced from progressively smaller volumes (see, e.g., Zhao, Bower, & Goss 2001; Genzel et al. 2003; Baganoff et al. 2001; Melia, Jokipii, & Narayanan 1992). The variable component of the near-IR (NIR) to X-ray emission fluctuates on a time scale of a few minutes (Porquet et al. 2003; Ghez et al. 2004) and exhibits a quasi-periodic modulation during some long duration flares (Genzel et al. 2003; Belanger et al. 2005), hinting at an origin within an accretion torus with size equal to a few Schwarzschild radii ($r_S \equiv 2GM/c^2 \simeq 10^{12}$ cm; Liu, Melia, & Petrosian 2006). The spectral (Falcke et al. 1998) and polarization (Aitken et al. 2000; Bower et al. 2005) characteristics of the mm/sub-mm radiation suggest that these too are produced within such a region (Melia, Liu, & Coker 2000). The cm and longer wavelength emission, on the other hand, has to be produced on progressively larger scales to avoid being self-absorbed (Liu & Melia 2001). Recent observations by Bower et al. (2004) show that indeed Sagittarius A*'s photosphere has a radius $\sim 24r_S$ at 7 mm.

In earlier work (Liu, Petrosian, & Melia 2004, hereafter LPM04), we showed that the stochastic acceleration (SA) of electrons interacting resonantly with plasma waves or turbulence generated via an MHD dissipation process (see, e.g., Miller, LaRosa, & Moore 1996; Hamilton & Petrosian 1992; Petrosian & Liu 2004), can produce the nonthermal particles emitting much of Sagittarius A*'s spectrum (see, e.g., Zhao, Bower, & Goss 2001; Genzel et al. 2003; Baganoff et al. 2001). This mechanism, originally invoked to explain how magnetic reconnection can energize particles during solar flares, can also accelerate electrons in the magnetized Keplerian accretion torus within $\sim 5 - 10 r_S$ of the black hole via a turbulence induced by the magneto-rotational instability (Balbus & Hawley 1991; Melia, Liu, & Coker 2001; Hawley & Balbus 2002). The radiation emitted at the acceleration site can explain the mm/sub-mm and shorter wavelength observations of this source in both the quiescent and flaring states.

An interesting prediction of this model is that, under most circumstances (see Fig. 1 in LPM04), the time required for energetic electrons to escape from the acceleration site is comparable to the acceleration and synchrotron cooling time scales so that there would be a significant outflux of accelerated particles. The nonthermal “halo” or jet formed by the escaping electrons may contribute to the cm-wavelength emission farther out (see, e.g., Liu & Melia 2001; LPM04; Zhao et al. 2004). In concert with the acceleration of electrons within $\sim 5 - 10r_S$ of the black hole, protons are also energized. But as we shall show in this paper, their acceleration efficiency in this “gas-dominated” region (with Alfvén velocity v_A much less than the speed of light c) is not sufficient to produce an observationally important flux away from Sagittarius A* itself.

However, particles continue to be accelerated outside of the inner torus, as evidenced, e.g., by the intensity and scale of the 7-mm emission region. We will therefore here also consider the *in situ* SA of particles in a larger “magnetically” dominated ($v_A \simeq c$) volume (extending out as far as $\sim 20 - 30r_S$), and demonstrate that the conditions required to account for Sagittarius A*’s 7-mm emission are in fact equally suited to the rapid acceleration of protons that escape and interact with the ambient medium surrounding Sagittarius A* to produce γ -rays.

Recently, the Galactic center (GC) has been identified by three air Čerenkov telescopes at \sim TeV energies: Whipple (Kosack et al. 2004), CANGAROO (Tsuchiya et al. 2004) and, most recently and significantly, HESS (Aharonian et al. 2004). The HEGRA ACT instrument has also put a (weak) upper limit on GC emission at 4.5 TeV (Aharonian et al. 2002) and the Milagro water Čerenkov extensive air-shower array has released a preliminary finding of a detection at similar energies from the region defined as $l \in \{20^\circ, 100^\circ\}$ and $|b| < 5^\circ$ (Fleysher 2002). We examine here the likelihood of these TeV photons being produced by the relativistic protons escaping the SA site near Sagittarius A*, and concentrate on the HESS results, though it should be noted that all of these observations lend crucial support to the notion that acceleration of particles to very high energies is taking place near (or at) the black hole. Observations pertinent to these high energy processes are described in § 2. In § 3 we discuss the acceleration of electrons and protons by turbulence and the observational constraints on the magnetic field and gas density of an acceleration region roughly $20r_S$ in size. The process of production of TeV photons is described in § 4 and a summary is presented in § 5.

2. Contextual Background

HESS detected a signal from the Galactic center in observations conducted over two epochs (June/July 2003 and July/August 2003) with a $\sim 6 - 9\sigma$ excess evident over this period. These data can be fitted by a power law with a spectral index 2.21 ± 0.09 , with a total flux above the instrument’s 165 GeV threshold of $(1.82 \pm 0.22) \times 10^{-7} \text{ m}^{-2} \text{ s}^{-1}$ (there is also a 15-20% error from the energy resolution uncertainty).

Intriguingly, the HESS data are difficult to reconcile with the EGRET GC source 3EG J1746-2851 (generally ascribed to pp-induced neutral pion decay at GeV energies; Fatuzzo & Melia 2003). In a re-analysis of select data from the 3EG catalog (Hartmann et al. 1999), Hooper & Dingus (2002) have shown that the GC is excluded at the 99.9% confidence limit as the true position of 3EG J1746-2851. The HESS source, on the other hand, is coincident within $\sim 1'$ of Sagittarius A*, though its centroid is displaced roughly $10''$ (corresponding to about 0.4 pc at a distance $D = 8 \text{ kpc}$) to the East of the GC. In addition, an extrapolation of the EGRET spectrum into HESS’s range over-predicts (by a factor ~ 20) the TeV γ -ray flux of the GC source. Recently, Crocker et al. (2005), and Aharonian & Neronov (2005a, 2005b), among others, have undertaken a detailed examination of the possible theoretical consequences of these new high-energy observations of the Galactic center, and inferred that we are apparently dealing with two separate sources. Perhaps both are associated with the SNR Sagittarius A East, but given its angular proximity to Sagittarius A*, the TeV source could be associated with the black hole itself.

What is not yet clear, however, is how the TeV γ -rays are produced. Models that invoke pp-induced neutral pion decays close to the black hole must contend with the collateral emission at other wavelengths (Markoff, Melia, & Sarcevic 1999; Aharonian & Neronov 2005a) due to the secondary particles produced in the ensuing cascade. And because the inner $\sim 10 r_S$ -emitting region of Sagittarius A* has received extensive scrutiny over the years (see, e.g., Melia, 1992; Falcke et al. 1998; Bromley et al. 2001; Yuan, Quataert, & Narayan 2003; Melia & Falcke 2001; Melia 2006), non-hadronic models face similar difficulties in satisfying the constraints imposed across Sagittarius A*’s broadband spectrum—from radio waves to X-rays and γ -rays (but see Atoyan & Dermer 2004 for a description of the “plerion” scenario, which avoids this complication). In the model we are proposing here, however, pp scattering events are quite rare in the acceleration site since the ambient proton density is very low. Instead, most of the accelerated protons diffuse out of the system and scatter with the ISM surrounding the black hole.

Our understanding of the circum-black-hole environment at the GC has improved considerably in recent years, thanks to observations with *Chandra* and detailed hydrodynamic modeling of the diffuse X-ray emission it detected within $r \sim 10''$ of Sagittarius A*. The hot

plasma producing this radiation, estimated at $\approx 7.6 \times 10^{31}$ ergs s $^{-1}$ arcsec $^{-2}$ in the 2–10 keV band, has an RMS electron density $\langle n \rangle \approx 26 \eta_f^{-1/2}$ cm $^{-3}$ and a temperature $k_B T \approx 1.3$ keV, with a total inferred mass of $\approx 0.1 M_\odot \eta_f^{1/2}$ (Baganoff et al. 2003), where η_f is the volume filling factor. We now understand that this hot gas is produced via collisions of winds of stars in the central cluster injected into the mini-cavity with a total mass rate of $\dot{M} \simeq 3 \times 10^{-3} M_\odot$ yr $^{-1}$ (Rockefeller et al. 2004). In the most recent census, some 25 bright, young wind sources have been identified and their mutual interactions account for the entire X-ray flux observed with *Chandra*. For a typical wind velocity $v = 1000$ km s $^{-1}$, the average (pre-shock) gas density in the central ~ 1 pc region is $\langle n_0 \rangle \sim 200$ cm $^{-3}$. We therefore have a good handle on the physical conditions in this region. In addition, this medium appears to be threaded by a rather strong magnetic field $\sim 0.1 - 1$ mG (Yusef-Zadeh et al. 1996), through which the escaping relativistic protons must diffuse. Note that this measured magnetic field is roughly in equipartition with the gas.

3. The Acceleration Site

To date, the most reliable measurement of Sagittarius A*’s intrinsic size has been made with closure amplitude imaging using the VLBA (Bower et al. 2004). At a wavelength of 7 mm, the source is confined to the inner ~ 24 Schwarzschild radii, though the size is variable on a time scale of hours to weeks and sometimes reaches $\sim 60 r_S$. Correspondingly, Sagittarius A*’s average flux density at this wavelength is ≈ 1.5 Jy (e.g., Falcke et al. 1998). These set strict constraints on the SA model, because the acceleration must not only be confined to a region of known size ($\sim 24 r_S$), but must also produce a particle distribution that accounts for the measured radiative output at this wavelength.

A complete treatment of SA by waves requires a solution of the coupled kinetic equations for the pitch-angle-averaged particle distribution $N(E, t)$ and the wave spectrum $\mathcal{W}(\mathbf{k})$:

$$\frac{\partial N}{\partial t} = \frac{\partial}{\partial E} \left[D_{EE} \frac{\partial N}{\partial E} - (A - \dot{E}_L) N \right] - \frac{N}{T_{\text{esc}}} + \dot{Q}, \quad (1)$$

$$\frac{\partial \mathcal{W}(\mathbf{k}, t)}{\partial t} = \dot{Q}_{\mathcal{W}}(\mathbf{k}, t) - \Gamma(\mathbf{k}) \mathcal{W}(\mathbf{k}, t) + \frac{\partial}{\partial k_i} \left[D_{ij} \frac{\partial}{\partial k_j} \mathcal{W}(\mathbf{k}, t) \right] - \frac{\mathcal{W}(\mathbf{k}, t)}{T_{\text{esc}}^{\mathcal{W}}(\mathbf{k})}, \quad (2)$$

where $E = \gamma - 1$, γ and \mathbf{k} are, respectively, the particle kinetic energy in units of the rest mass energy, Lorentz factor and the wave vector. The loss rate, the source and escape terms for the particles are given by \dot{E}_L , \dot{Q} and $N(E)/T_{\text{esc}}$, respectively. The terms on the right-hand-side of Equation (2) represent the wave generation, damping, cascade, and leakage processes. The energy diffusion coefficient $D_{EE}(E)$ and the function $A(E) = (D_{EE}/E)(2 - \gamma^{-2})/(1 + \gamma^{-1})$

depend on $\mathcal{W}(\mathbf{k})$, and the wave damping rate $\Gamma(\mathbf{k})$ depends on $N(E)$. That is how the equations are coupled.

SA of particles is dominated by the transit-time damping and cyclotron-resonance processes. Recent progress in studying the scattering and acceleration of charged particles by MHD turbulence indicates that fast mode waves play the dominant role (Yan & Lazarian 2002). Fast wave turbulence is isotropic and has a power-law spectrum with an index of $q = 1.5$ in the inertial range (Cho, Lazarian & Vishniac 2002). At small scales, the waves are subjected to collisionless damping, which depends on the wave propagation angle with respect to the magnetic field θ (Stepanov 1958; Ginzburg 1961; Petrosian, Yan, & Lazarian 2005):

$$\Gamma(\mathbf{k}) \simeq u(\pi\beta_p\delta)^{1/2} \frac{kv_A \sin^2 \theta}{2 \cos \theta}, \quad \text{for } 1 \gg \beta_p \gg \delta, \quad (3)$$

where u , $\delta = m_e/m_p$, and $\beta_p = 4\pi P_{\text{gas}}/B^2$ are the ratio of the proton to electron energy density, the electron to proton mass, and the gas to magnetic field pressure, respectively. The wave spectrum will cut off when this damping rate dominates the cascade rate $\tau_{\text{cas}}^{-1}(k) \simeq v_A f_{\text{turb}}(k_{\text{min}}k/2\pi)^{1/2}$, where $2\pi/k_{\text{min}}$ gives the turbulence injection length scale and $f_{\text{turb}} = [8\pi \int \mathcal{W}(k)dk]/B^2 < 1$ is the ratio of the turbulence to magnetic field energy density. Most of the waves at small scales therefore propagate along the magnetic field line with the propagation angle $\theta < \theta_{\text{cr}}(k) = (2f_{\text{turb}}^2 k_{\text{min}}/\pi^2 u^2 \beta_p \delta k)^{1/4}$. To study particle acceleration by such turbulence, one may represent the latter as parallel propagating waves with spectrum $\mathcal{W} \propto k^{-3/2} \theta_{\text{cr}}^2 \propto k^{-2}$.

Almost all of the observed emission from the direction of Sagittarius A* is produced by nonthermal relativistic particles ($E \simeq \gamma \gg 1$ and $A \simeq 2D_{EE}/E$). As such, the characteristic interaction time τ_p , the pitch-angle-averaged scattering ($\tau_{\text{sc}} \equiv \langle [1 - \mu^2]^2 / D_{\mu\mu} \rangle$) and acceleration ($\tau_{\text{ac}} \equiv E^2 / D_{EE}$) times, and the escape time, can all be expressed in units of $\tau_{\text{tr}} \equiv R/c$, the light transit time for an acceleration region of size R (Dung & Petrosian 1994; Petrosian & Liu 2004):

$$\tau_p = \frac{4}{\pi(q-1)f_{\text{turb}}\Omega} \left(\frac{ck_{\text{min}}}{\Omega} \right)^{1-q} \simeq 1.3 \frac{\tau_{\text{tr}}}{(q-1)f_{\text{turb}}Rk_{\text{min}}} \left(\frac{ck_{\text{min}}}{\Omega} \right)^{2-q}, \quad (4)$$

$$\tau_{\text{sc}} \simeq \tau_p \gamma^{2-q} \simeq 1.3 \frac{\tau_{\text{tr}}}{(q-1)f_{\text{turb}}Rk_{\text{min}}} \left(\frac{\gamma ck_{\text{min}}}{\Omega} \right)^{2-q}, \quad (5)$$

$$\tau_{\text{ac}} \simeq \frac{2(\beta_A^2 + 1)\tau_p}{\beta_A^2} \gamma^{2-q} \simeq \frac{2.6(\beta_A^2 + 1)}{\beta_A^2} \frac{\tau_{\text{tr}}}{(q-1)f_{\text{turb}}Rk_{\text{min}}} \left(\frac{\gamma ck_{\text{min}}}{\Omega} \right)^{2-q}, \quad (6)$$

$$T_{\text{esc}} = \frac{\tau_{\text{tr}}^2}{\tau_{\text{sc}}} + 2^{1/2} \tau_{\text{tr}} \simeq \left[0.8(q-1)f_{\text{turb}}Rk_{\text{min}} \left(\frac{\gamma ck_{\text{min}}}{\Omega} \right)^{q-2} + 1.4 \right] \tau_{\text{tr}}, \quad (7)$$

where μ , $D_{\mu\mu}$, and Ω are, respectively, the cosine of the particle pitch angle with respect

to the large scale magnetic field B , the pitch angle scattering rate, and the nonrelativistic gyrofrequency of the particles, and $2\pi/k_{\min} \lesssim R$. The (dimensionless) Alfvén velocity is defined as

$$\beta_A \equiv \frac{B}{(4\pi n m_p c^2)^{1/2}} = 7.3 \left(\frac{B}{1\text{G}} \right) \left(\frac{n}{1\text{cm}^{-3}} \right)^{-1/2} \simeq \frac{v_A/c}{[1 - (v_A/c)^2]^{1/2}}. \quad (8)$$

Note that, for $\beta_A \geq 1$, the phase velocity of the waves is $v_A/c = w/(ck) \simeq \beta_A/(1 + \beta_A^2)^{1/2}$.

For $q = 2$, the acceleration and escape time scales become energy independent. When the loss processes are unimportant (i.e., $\dot{E}_L \ll A$), Equation (1) can be reduced to

$$\frac{\partial N}{\partial t} = \frac{\partial}{\partial E} \left[E^2 \frac{\partial N}{\partial E} - 2EN \right] - \frac{N}{T_{\text{esc}}} + \dot{Q}, \quad (9)$$

whose steady-state solution is $N \propto E^{-p}$ above the particle injection energy, where the spectral index p is determined by the ratio of τ_{ac} to T_{esc} :

$$p = \left(\frac{9}{4} + \frac{\tau_{\text{ac}}}{T_{\text{esc}}} \right)^{1/2} - 0.5 > 1.0. \quad (10)$$

There are four primary parameters in the SA model (LPM04): R , $f_{\text{turb}} R k_{\min}$, n and B . For Sagittarius A*, $R \simeq 20r_S$ at the wavelength of interest (i.e., 7 mm). The observed γ -ray spectral index and the radio to IR spectrum set strict constraints on the other three. To produce a power-law spectrum of relativistic protons with $p = 2.2$, which gives rise to a γ -ray spectral index of the same value via pp scattering processes, Equations (10) and (7) show that $\tau_{\text{ac}} \simeq 5.0 T_{\text{esc}} = (4f_{\text{turb}} R k_{\min} + 7)\tau_{\text{tr}}$. Combining this with Equation (6), one has

$$\beta_A = \left(\frac{2.6}{4[f_{\text{turb}} R k_{\min}]^2 + 7f_{\text{turb}} R k_{\min} - 2.6} \right)^{1/2}. \quad (11)$$

Since $f_{\text{turb}} \leq 1$, this sets a constraint on β_A .

Next we consider the constraints imposed on B and n by the 7 mm observations. The turbulence discussed above accelerates both protons and electrons to a power-law distribution with $p = 2.2$ in the relativistic energy range. The source of electrons for this process is likely the hot flow accreting toward the black hole. We therefore assume that the injected electrons have a mean Lorentz factor $\gamma_{\text{in}} = 10$. So the electron distribution has a rising spectrum below this energy and a power-law spectrum above it (Park & Petrosian 1995). The distribution cuts off when the synchrotron cooling time

$$\tau_{\text{syn}} = \frac{9m_e^3 c^5}{4e^4 B^2 \gamma} = 78 \left(\frac{B}{100\text{G}} \right)^{-2} \left(\frac{\gamma}{10^3} \right)^{-1} \text{ s} \quad (12)$$

equals the acceleration time $\tau_{\text{ac}} = 5.0T_{\text{esc}} = 670(4f_{\text{turb}}Rk_{\text{min}} + 7)(R/20r_S)$ s. Here, m_e is the electron mass and e is its charge. One therefore gets a high-energy cutoff

$$\gamma_M = \frac{17}{1 + 0.6f_{\text{turb}}Rk_{\text{min}}} \left(\frac{B}{100\text{G}}\right)^{-2} \left(\frac{R}{20r_S}\right)^{-1}. \quad (13)$$

The corresponding frequency of the synchrotron emission is

$$\nu_M = \frac{3eB\gamma_M^2}{4\pi m_e c} = 120 \left(\frac{1}{1 + 0.6f_{\text{turb}}Rk_{\text{min}}}\right)^2 \left(\frac{B}{100\text{G}}\right)^{-3} \left(\frac{R}{20r_S}\right)^{-2} \text{GHz}, \quad (14)$$

which should be higher than the observed frequency 43 GHz. We choose $\nu_M \geq 60$ GHz (which is 40% above the observed value), giving

$$B \leq 126 \left(\frac{R}{20r_S}\right)^{-2/3} \left(\frac{1}{1 + 0.6f_{\text{turb}}Rk_{\text{min}}}\right)^{2/3} \text{G} < 126 \left(\frac{R}{20r_S}\right)^{-2/3} \text{G}. \quad (15)$$

This constraint is indicated by the vertical line in Figure 1.

Because Sagittarius A* has a flat radio spectrum with $\alpha \simeq -0.3$ ($F_\nu \propto \nu^{-\alpha}$), the optical depth of this nonthermal source at 7 mm τ_0 has to be ~ 1 to avoid producing emission in excess of the observed flux below (for $\tau_0 < 1$) or above (for $\tau_0 > 1$) 7 mm. We require $30\text{GHz} \leq \nu_0 \leq 60\text{GHz}$, where $\tau_0(\nu_0) = 1$ for a source extent of $R = 20r_S$, i.e. (Pacholczyk 1970)

$$0.08 \leq \left(\frac{n}{10^3\text{cm}^{-3}}\right) \left(\frac{\gamma_{\text{in}}}{10}\right)^{1.2} \left(\frac{B}{100\text{G}}\right)^{2.1} \left(\frac{R}{20r_S}\right) \leq 0.68, \quad (16)$$

which excludes the lower-left and upper-right portions of the $B - n$ plane (Fig. 1). The luminosity associated with this emission (assuming a spherical source) would be given by (Pacholczyk 1970)

$$\nu_M L_\nu(\nu_M) = 4.9 \times 10^{34} \left(\frac{n}{10^3\text{cm}^{-3}}\right) \left(\frac{\gamma_{\text{in}}}{10}\right)^{1.2} \left(\frac{B}{100\text{G}}\right)^{0.4} \left(\frac{R}{20r_S}\right)^{2.2} \left(\frac{1}{1 + 0.6f_{\text{turb}}Rk_{\text{min}}}\right)^{0.8} \text{ergs s}^{-1}, \quad (17)$$

which must be lower than the radio to NIR luminosity of $\sim 5 \times 10^{34}$ ergs s⁻¹. In combination with Equation (11), this constraint excludes the upper portion of the $B - n$ plane (Fig. 1). Therefore, to reconcile the radio to IR and γ -ray emissions with the SA model, the plasma must be strongly magnetized with $\beta_A > 1$. The blank region near the middle of Figure 1 shows the allowed parameter space, when all these constraints are taken into account. The exact properties of the plasma required to explain the 7 mm observations depend on the source structure and geometry. As an illustration, we consider a uniform spherical model

with radius $R = 20 r_S$ (roughly consistent with the VLBA measurement). Calculating the accelerated electron spectrum and consequent radio emission yields a best fit model for the 7 mm data (with $B = 70$ G, $n = 600 \text{ cm}^{-3}$, and $f_{\text{turb}} R k_{\text{min}} = 0.016$) corresponding to the black dot near the middle of Figure 1.

Now, in concordance with the acceleration of electrons to produce Sagittarius A*’s 7 mm emission, protons are also energized. Figure 2 shows the acceleration and escape time scales for electrons (*thin*) and protons (*thick*) in plasmas with $\beta_A = 0.15$ and 2.0. The time scales are given in units of τ_{tr} , and we assume $f_{\text{turb}} R k_{\text{min}} = 2\pi$ for this calculation. In the general case, $\tau_{\text{ac}} \propto \tau_{\text{sc}} \propto f_{\text{turb}}^{-1} \geq 1$. From these time scales, we see that a hard high energy proton spectrum can only be produced in plasmas with $\beta_A \geq 0.15$ and low-energy protons have an escape time much longer than their acceleration time. Thus, most of these particles are energized efficiently to about $E_{\text{min}} \sim 300$ MeV, above which the acceleration and escape times become comparable and the protons attain a power-law distribution. For such a spectrum, we have $N(E) = (p - 1) n E_{\text{min}}^{p-1} E^{-p}$, where we have used the fact that the high cutoff energy $E_{\text{max}} \simeq 2\pi e B / k_{\text{min}} = 4.2 \times 10^{17}$ eV is much larger than the ‘turnover’ energy E_{min} . The ensuing energy flux associated with protons with $E \geq E_o = 0.1$ TeV is given by

$$\begin{aligned} F_p &= \frac{p - 1}{p - 2} \frac{V n E_{\text{min}}^{p-1} E_o^{2-p}}{T_{\text{esc}}} & (18) \\ &= 3.2 \times 10^{37} \left(\frac{n}{10^3 \text{cm}^{-3}} \right) \left(\frac{E_{\text{min}}}{300 \text{MeV}} \right)^{1.2} \left(\frac{E_o}{0.1 \text{TeV}} \right)^{-0.2} \left(\frac{3V}{4\pi R^3} \right) \left(\frac{R}{20 r_S} \right)^2 \text{ ergs s}^{-1}. \end{aligned}$$

With all other parameters being fixed, F_p only depends on n , and is shown on the right axis of Figure 1. Note that the illustrative uniform spherical model for the 7 mm observations of Sagittarius A* (introduced above) corresponds to a proton energy flux $F_p \approx 1.9 \times 10^{37}$ ergs s^{-1} . The total power associated with the proton flux is $\sim 6.0 \times 10^{37}$ erg s^{-1} . The power injected into the fast wave turbulence can be estimated as $\sim (4\pi/3) R^2 v_A B^2 f_{\text{turb}}^2 \sim 6.0 \times 10^{37}$ ergs s^{-1} . Most of the dissipated turbulence energy then goes into the protons. And for the model parameters $\theta_{\text{cr}} < 0.5$ for $k > k_{\text{min}}$ (note that $u \sim E_{\text{min}} / \gamma_{\text{in}} m_e c^2 \simeq 60$), the approximation of the turbulence as parallel propagating waves is therefore appropriate.

4. The PP Interaction Region

Once the relativistic protons leave the acceleration site, they diffuse through the medium surrounding Sagittarius A*, as described in § 2 above. The transport of cosmic rays through chaotic magnetic fields has been considered by several authors, among them Giacalone and Jokipii (1999), and Casse, Lemoine, and Pelletier (2001). These particles effectively execute

a random walk through the ISM with a mean free path $c\tau_{\text{sc}}$. There is no evidence of a large scale magnetic field on the extension corresponding to the HESS point-spread-function. In addition, no structure has been detected within the mini-cavity on angular scales referenced to *Chandra*'s spatial resolution of ~ 1 arcsec. Even more constraining are the numerical simulations for the diffuse X-ray emission, which show that shocks resulting from wind-wind collisions are typically ten times smaller than the separation between stars. This corresponds roughly to a coherence scale $\sim 10^{16}$ cm. We therefore infer that $f_{\text{turb}} \simeq 1$ and $k_{\text{min}} \simeq 6 \times 10^{-16}$ cm $^{-1}$. Because the temperature of the ambient gas is low ($\beta_p \sim 1$), the damping of fast mode waves interacting with relativistic protons is unimportant. The turbulence is isotropic with $q = 3/2$ up to k_{cr} , which can be estimated with $\theta_{\text{cr}}(k_{\text{cr}}) = 1$. We therefore have $k_{\text{cr}} \simeq 400k_{\text{min}}/\beta_p$.

Combined with Equation (5), this therefore yields a scattering time in this region surrounding Sagittarius A* of $\tau_{\text{sc}} \simeq 6.4 \times 10^4 (E/10 \text{ TeV})^{1/2} (B/0.1 \text{ mG})^{-1/2}$ s. The HESS source may be as large as $R = 3$ pc (Aharonian et al. 2004; Aharonian & Neronov 2005b). Thus, the total path length of a relativistic proton in the medium surrounding Sagittarius A* is $l_{\text{tot}} = R^2/(\tau_{\text{sc}}c) \simeq 4.5 \times 10^{22} (E/10 \text{ TeV})^{-1/2} (B/0.1 \text{ mG})^{1/2}$ cm. On the other hand, the cross section σ_{pp} for pp scattering is weakly dependent on energy, and may be taken as ~ 40 mb in the energy range of interest (see, e.g., Crocker et al. 2004). Therefore the mean free path for a pp scattering event is $\sim [\langle n_0 \rangle \sigma_{pp}]^{-1} \approx 1.3 \times 10^{23} [\langle n_0 \rangle / 200 \text{ cm}^{-3}]^{-1}$ cm, so $l_{\text{tot}} \langle n_0 \rangle \sigma_{pp} \sim O(1)$. In other words, most of the escaping relativistic protons scatter with background protons about once in the wind-shocked medium surrounding Sagittarius A*. Because the corresponding pp scattering time is $\sim 10^5$ yrs, which is longer than the time required for the wind-injected ISM to reach equilibrium (Rockefeller et al. 2004), any variability in the TeV emission would be associated primarily with density fluctuations on large spatial scales, rather than changes in the source. We would expect the source to be stable on a time scale of a year or less.¹

The particle cascade generated by scatterings between the relativistic protons diffusing away from the acceleration site and protons in the ambient medium produces additional spectral components due to neutral pion decays and emission by secondary leptons. Neutral pion decays produce a γ -ray spectrum that dominates above ~ 100 MeV. At lower energies, most of the radiative emission is due to the decay products of charged pions. These leptons radiate via synchrotron, bremsstrahlung, and inverse Compton scattering with the strong UV and IR fields bathing the inner few parsecs of the Galaxy (Telesco, Davidson & Werner

¹Equation (6) shows that the corresponding acceleration time in this region is $\tau_{\text{ac}} \simeq 7.5 \times 10^8 \tau_{\text{sc}} (\langle n_0 \rangle / 200 \text{ cm}^{-3}) (B/0.1 \text{ mG})^{-2}$, which is longer than any other relevant time scales, so the acceleration of protons by the turbulence outside of Sagittarius A* itself may be ignored.

1996; Davidson et al. 1992; Becklin, Gatley & Werner 1982). A detailed description of how the total emission from these various processes can be calculated appears in Fatuzzo & Melia (2003). For a proton energy flux $F_p \approx 1.6 \times 10^{37}$ ergs s^{-1} (above 300 MeV with $p = 2.25$), the broadband spectrum resulting from these processes is shown in Figure 3. For this calculation, we assume that the protons are scattered only once and the magnetic field strength in the pp interaction zone was set at 1.0 mG. The currently available data (or upper limits) are also shown here for comparison with our model. We also include the GLAST single energy sensitivity for a one-year all-sky survey, which shows that the HESS ~ 100 MeV–100 GeV counterpart may also be detectable. Note that since cooling time of TeV electrons and positrons in the pp interaction region is considerably shorter than the pp scattering time ($\sim 4 \times 10^{12}$ s), their distributions reach a cooling broken-power spectrum in the steady-state.

The spectrum fits the HESS data and is consistent with observations in other lower energy bands. The fact that the required proton power is more than 3 times below that predicted from the fitting of the 7 mm data ($\sim 6.0 \times 10^{37}$ ergs s^{-1}) indicates that most of the protons diffuse beyond the HESS point-spread-function, which may explain the recently observed diffusion gamma-ray emission from the Galactic Center (Aharonian et al. 2006), constituting one of the strongest arguments in favor of the SA model for the origin of Sagittarius A*’s spectrum.

5. Conclusion and Discussion

The combination of a reliable intrinsic source size measurement of Sagittarius A* at 7 mm with the detection of TeV emission from its vicinity has important implications for the acceleration of relativistic particles near the black hole. We have shown that SA of electrons and protons in a magnetic field dominated plasma can account for both the 7 mm observations via *in situ* electron synchrotron process and the HESS observations through the diffusion of accelerated protons into the surrounding ISM. The fact that a medium with $\beta_A > 1$ is required is intriguing in light of recent MHD simulations of black hole accretion (Hawley & Balbus 2002; Hirose et al. 2004). These numerical calculations show that there are always magnetic-field-dominated coronas above the disk and funnels along its symmetry axis. These regions may be the electron and proton acceleration sites. Speculating further, our results may also be in line with current concepts of a Poynting flux dominated outflow, driven either by an accretion torus or by a spinning black hole (Camenzind 2004; Semenov, Dyadechkin, & Punsly 2004; Nakamura & Meier 2004).

Although we suggested that most of the protons producing the TeV emission scatter

at least once within a region corresponding to the HESS point-spread-function, given the uncertainties in the observed properties of the ISM, it is still possible that a significant fraction of very high energy protons diffuse outward to even larger radii. Then the proton spectral index in the acceleration region would need to be smaller than 2.2 in order to explain the HESS photon spectrum since the proton scattering time increases with energy. However, the difference between the proton and photon spectral indexes, which depends on the energy-dependent diffusion of the former, is expected to be small (Aharonian & Neronov 2005b), and our main conclusions still hold. In this paper we studied the SA of particles interacting with parallel propagating waves. This may not be true at the wave injection scale where the turbulence could be isotropic. A comprehensive investigation of this aspect will be presented in a separate paper.

We have shown above that particles energized in a magnetized plasma apparently produce most of Sagittarius A*’s emission. This may very well be the case for the accretion flow in many other compact objects. A thorough investigation of the SA model for particles in a magnetic field dominated outflow will also play an important role in bridging the above mentioned theoretical developments with observations. Eventually, studying SA in such compact environments may also reveal the nature of large scale relativistic jets, where the coupling of plasma turbulence to the energetic particles could be very strong.

The radiative consequences of relativistic protons in active galactic nuclei and their implications on the formation of large scale jets have been studied extensively during the past few decades (Begelman, Rudak, & Sikora 1990; Atoyan & Dermer 2003). With the theory of SA developed here, properties of the turbulent plasma responsible for the proton acceleration can be inferred. The constraints to the particle acceleration processes would be stricter should the acceleration of electrons by the same turbulence be also considered, as is the approach we took here in modeling the broadband spectrum of Sagittarius A*.

We have used the spatially integrated results of SA as a first order approximation in the previous investigations. However, to model spatially resolved sources, one must take into account the source structure. Monte Carlo simulations of SA may be a good approach in such cases and this will likely be the next step in the development of our model. For a complete treatment of SA, the properties of the waves must also be addressed. MHD simulations provide a complementary vehicle for this problem and when combined with the SA theory, can yield a global picture of energy dissipation channeled via turbulence. Investigations of this kind will be fruitful in providing a better understanding of many nonthermal astrophysical sources. With little modification, the model can also be applied to other astrophysical systems where the plasma is collisionless and strong turbulence presents. The observed emission spectra can be used to determine the properties of the plasma and

to reveal the underlying physics processes.

FM thanks Ray Volkas and Roland Crocker for very helpful discussions. SL is supported by the Director’s Fellowship at LANL. This research was partially supported by NSF grant ATM-0312344, NASA grants NAG5-12111, NAG5 11918-1 (at Stanford), and NSF grant AST-0402502 (at Arizona). FM is very grateful to the University of Melbourne for its support (through a Miegunyah Fellowship), and MF is supported by the Hauck Foundation through Xavier University.

REFERENCES

- Aharonian, F. A. and Neronov, A. 2005a, *ApJ*, 619, 306
- Aharonian, F. A. and Neronov, A. 2005b, *ApSS*, 300, 255
- Aharonian, F. A. et al. 2006, *Nature*, 439, 695
- Aharonian, F. A. et al. 2004, *A&A*, 425, 13
- Aharonian, F. A. et al. 2002, *A&A*, 395, 803
- Aitken, D. K., Greaves, J., Chrysostomou, A., Jenness, T., Holland, W., Hough, J. H.,
Pierce-Price, D., & Ricker, J. 2000, *ApJ*, 534, L173
- Atoyan, A. M. and Dermer, C. D. 2003, *ApJ*, 586, 79
- Atoyan, A. M. and Dermer, C. D. 2004, *ApJ*, 617, L123
- Baganoff, F. K. et al. 2001, *Nature*, 413, 349
- Baganoff, F. K. et al. 2003, *ApJ*, 591, 891
- Balbus, S. A. and Hawley, J. F. 1991, *ApJ*, 376, 214
- Bélangier, G. et al. 2005, *ApJ*, 635, 1095
- Begelman, M. C., Rudak, B., and Sikora, M. 1990, *ApJ*, 362, 38
- Bromley, B., Melia, F., and Liu, S. 2001, *ApJ*, 555, L83
- Bower, G. C., et al. 2004, *Science*, 304, 704
- Bower, G. C., Falcke, H., Wright, M. C. H., & Backer, D. C. 2005, *ApJ*, 618, 29
- Camenzind, M. 2004, *astro-ph/0411573*
- Casse, F., Lemoine, M., and Pelletier, G. 2001, *Phys. Rev. D*, 64, 023002-1
- Cho, J., Lazarian, A., & Vishniac, T. 2002, *astro-ph/0205286*
- Crocker, R., Fatuzzo, M., Jokipii, R., Melia, F., and Volkas, R. 2005, *ApJ*, 622, L37
- Dung, R., & Petrosian, V. 1994, *ApJ*, 421, 550
- Falcke, H. et al. 1998, *ApJ*, 499, 731

- Fatuzzo, M. and Melia, F. 2003, *ApJ*, 596, 1035
- Fleysher, R. and Milagro Collaboration 2002, *Bulletin of the American Astronomical Society*, 34, 676
- Ginzburg, V. L. 1961, *Propagation of Electromagnetic Waves in Plasma* (New York: Gordon & Breach)
- Genzel, R., et al. 2003, *Nature*, 425, 934
- Ghez, A. M., et al. 2003, *ApJ*, 586, L127
- Ghez, A. M., et al. 2004, *ApJ*, 601, L159
- Giacalone, J. and Jokipii, J. R. 1999, *ApJ*, 520, 204
- Hamilton, R. J. and Petrosian, V. 1992, *ApJ*, 398, 350
- Hartman, R. C. et al. 1999, *ApJS*, 123, 79
- Hawley, J. F., and Balbus, S. A. 2002, *ApJ*, 573, 738
- Hirose, S., Krolik, J. H., De Villiers, J. P., & Hawley, J. F. 2004, *ApJ*, 606, 1083
- Hooper, D., and Dingus, B. 2002, *astro-ph/0212509*
- Kosack, K. and Collaboration, t. V. 2004, *astro-ph/0403422*
- Liu, S. and Melia, F. 2001, *ApJ*, 561, L77
- Liu, S., Petrosian, V., and Melia, F. 2004, *ApJ*, 611, L101
- Liu, S., Melia, F., and Petrosian, V. 2006, *ApJ*, 636, 798
- Markoff, S., Melia, F., and Sarcevic, I. 1999, *ApJ*, 522, 870
- Mayer-Hasselwander, H. A., et al. 1998, *ã*, 335, 161
- Melia, F. 1992, *ApJ*, 387, L25
- Melia, F. 2006, *The Galactic Center Supermassive Black Hole* (Princeton: New York)
- Melia, F. and Falcke, H. 2001, *ARAA*, 39, 309
- Melia, F., Jokipii, J. R., & Narayanan, A. 2002, *ApJ*, 395, L87
- Melia, F., Liu, S., and Coker, R. 2000, *ApJ*, 545, L117

- Melia, F., Liu, S., and Coker, R. 2001, *ApJ*, 553, 146
- Miller, J. A., LaRosa, T. N., and Moore, R. L., 1996, *ApJ*, 461, 445
- Nakamura, M., and Meier, D. L. 2004, *ApJ*, 617, 123
- Pacholczyk, A. G. 1970, *Radio Astrophysics* (Freeman: San Francisco)
- Park, B. T., & Petrosian, V. 1995, *ApJ*, 446, 699.
- Petrosian, V. and Liu, S. 2004, *ApJ*, 610, 550
- Petrosian, V., Yan, H., & Lazarian, A. 2006, *ApJ*, in press. astro-ph/0508567
- Porquet, D., et al. 2003, *A&A*, 407, L17
- Rockefeller, G., Fryer, C. L., Melia, F., and Warren, M. S. 2004, *ApJ*, 604, 662
- Semenov, V., Dyadechkin, S., and Punsly, B. 2004, *Science*, 305, 978
- Schödel, R., Ott, R., Genzel, R., Eckart, A., Mouawad, N., and Alexander, T. 2003, *ApJ*, 596, 1015
- Stepanov, K. N., *Soviet JETP*, 34, 1292
- Tsuchiya, K. et al. 2004, *ApJ*, 606, L115
- Yan, H., & Lazarian, A. 2002, *Phys.Rev.Letters* 89, 281102-1
- Yuan, F., Quataert, E., and Narayan, R. 2005, *ApJ*, 598, 301
- Yusef-Zadeh, F., Roberts, D. A., Goss, W. M., Frail, D. A., and Green, A. J. 1996, *ApJ*, 466, L25
- Zhao, J.-H., Bower, G. C., and Goss, W. M. 2001, *ApJ*, 547, L29
- Zhao, J.-H. et al. 2004, *ApJ*, 603, L85

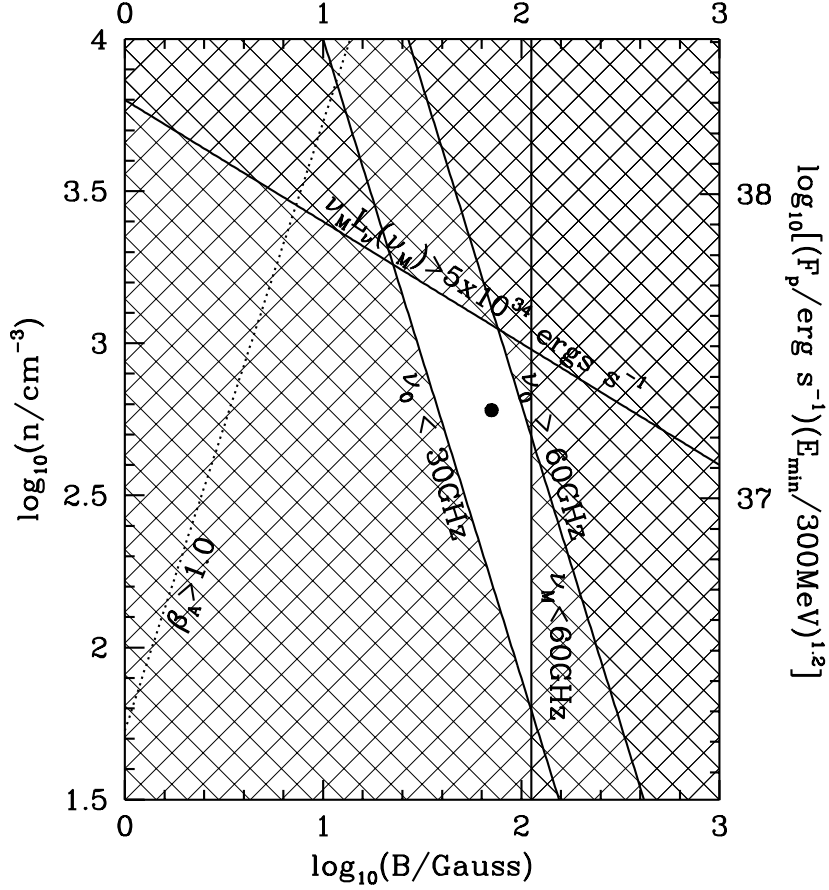


Fig. 1.— Constraints on the density and magnetic field of the acceleration site, where electrons produce the observed 7 mm emission while protons escape toward large radii and produce the HESS γ -ray signal via collisions with the ambient protons. Here we have assumed that $\gamma_{\text{in}} = 10$ and $R = 20 r_S$. The dashed line corresponds to $\beta_A = 1$. At 7 mm the source is optically thin (thick) in the lower-left (upper-right) portion of the figure. The constraint $B \lesssim 120$ G comes from the requirement that the synchrotron emission cuts off above 60 GHz. The upper area is excluded because the total synchrotron power from the acceleration site can not exceed the radio to IR luminosity of Sagittarius A*. Depending on the details of the source geometry, the 7 mm observations may be explained with B and n in the blank (central) region of this figure. For example, the black dot corresponds to an illustrative uniform sphere model. The right axis indicates the power in escaping protons with energy $E > 0.1$ TeV.

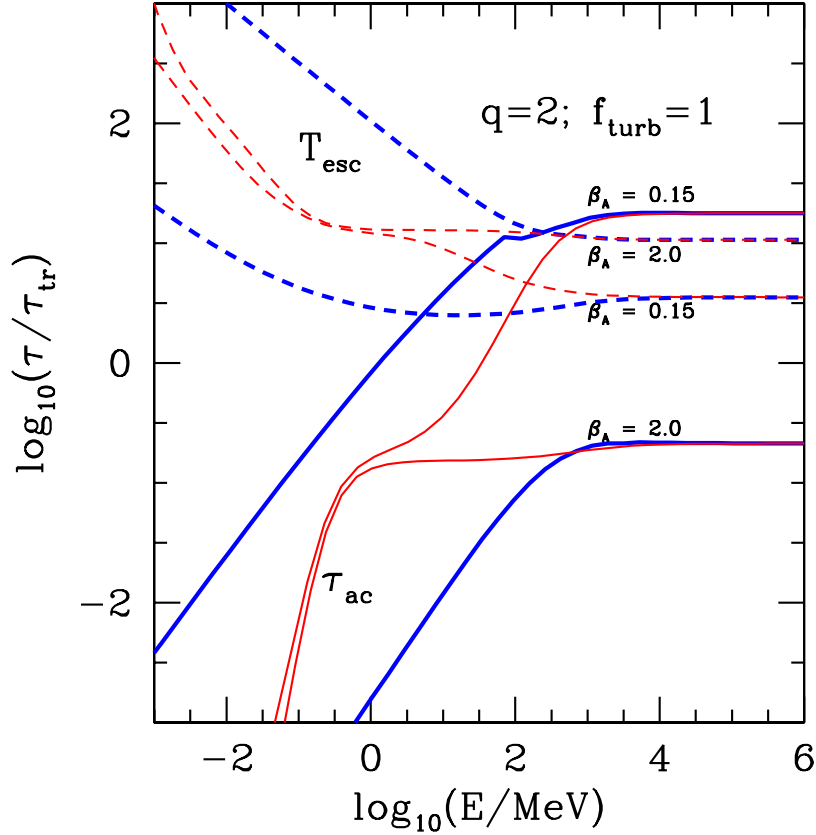


Fig. 2.— The acceleration (solid) and escape (dashed) time scales for electrons (thin) and protons (thick), in plasmas with $\beta_A = 0.15$ and 2.0 (indicated in the figure). The time scales are shown in units of the light transit time $\tau_{\text{tr}} = R/c$. The turbulence is assumed to be in energy equipartition with the magnetic field and $q = 2$. In a weakly magnetized plasma ($\beta_A < 1.0$), whistler waves can accelerate low-energy electrons to a Lorentz factor $\beta_A m_p/m_e$, causing a sharp rise in the electron acceleration time with energy beyond 1 MeV. The acceleration of nonrelativistic electrons is dominated by high frequency electromagnetic waves. In a strongly magnetized plasma ($\beta_A > 1.0$), the whistler wave branch vanishes, the acceleration time of relativistic electrons is almost energy-independent.

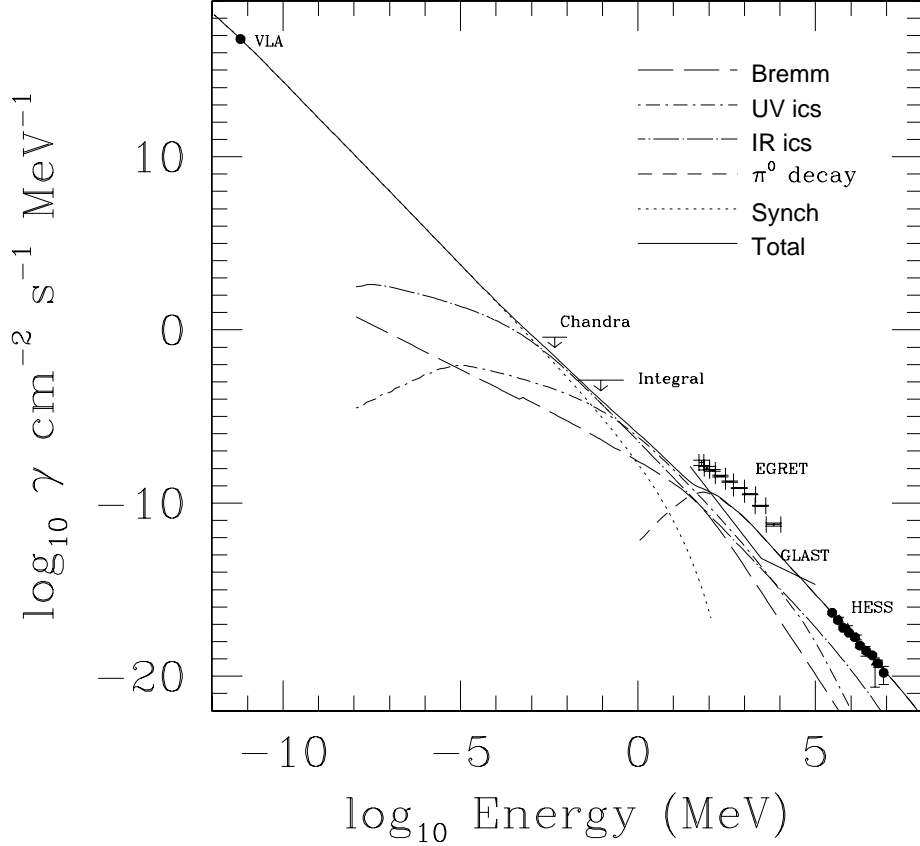


Fig. 3.— Broadband emission from the pp interaction zone due to (short dashed curve) neutral pion decays, and (long dashed curve) bremsstrahlung, (short dash-dot curve) UV inverse Compton scattering, (long dash-dot curve) IR inverse Compton scattering, and (dotted curve) synchrotron emission by the secondary leptons. The solid curve represents the total broadband emission. For comparison, we also show the currently available data (or upper limits), and the expected GLAST single energy sensitivity for a one-year all-sky survey. The Integral observations are from Belanger et al. (2005), the EGRET source 3EG J1746-2852 is from Mayer-Hasselwander et al. (1998), and the HESS observations are reported in Aharonian et al. (2004). The Chandra upper limit may be found in Rockefeller et al. (2004), and the VLA datum is reproduced in Fatuzzo and Melia (2003).